



## Scholars' Mine

---

Masters Theses

Student Theses and Dissertations

---

Summer 2010

### Multi axis slicing for rapid prototyping

Divya Kanakanala

Follow this and additional works at: [https://scholarsmine.mst.edu/masters\\_theses](https://scholarsmine.mst.edu/masters_theses)

 Part of the [Computer Sciences Commons](#)

Department:

---

#### Recommended Citation

Kanakanala, Divya, "Multi axis slicing for rapid prototyping" (2010). *Masters Theses*. 4990.  
[https://scholarsmine.mst.edu/masters\\_theses/4990](https://scholarsmine.mst.edu/masters_theses/4990)

This thesis is brought to you by Scholars' Mine, a service of the Missouri S&T Library and Learning Resources. This work is protected by U. S. Copyright Law. Unauthorized use including reproduction for redistribution requires the permission of the copyright holder. For more information, please contact [scholarsmine@mst.edu](mailto:scholarsmine@mst.edu).



# MULTI AXIS SLICING FOR RAPID PROTOTYPING

by

DIVYA KANAKANALA

A THESIS

Presented to the Faculty of the Graduate School of the

MISSOURI UNIVERSITY OF SCIENCE AND TECHNOLOGY

In Partial Fulfillment of the Requirements for the Degree

MASTER OF SCIENCE IN COMPUTER SCIENCE

2010

Approved by

Xiaoqing (Frank) Liu, Advisor  
Frank W. Liou, Co-Advisor  
Maggie Cheng



## ABSTRACT

With multi-axis capability, direct laser deposition process can produce a metal part without the usage of support structures. In order to fully utilize such a capability, a slicing method for multi-axis metal deposition process is discussed. Using the geometry information of adjacent layers, the slicing direction and layer thickness can be changed as needed. A hierarchy structure is designed to manage the topological information which is used to determine the slicing sequence. The parallel slicing process is studied to build hollow type structure. With such a character, the hole like feature can be deposited directly to save the required machining operation and material cost, which improves the efficiency of the metal deposition process. Combined with direct 3D layer deposition technique, the multi-axis slicing method is implemented.

## ACKNOWLEDGEMENTS

I would like to express my gratitude to my advisors, Dr. Frank Liu and Dr. Frank W. Liou for giving me the opportunity to work on this project. I am grateful to them for their advice and guidance at every point of this research and during the course of my Master's program. I would also like to thank Dr. Maggie Cheng for her time and effort in serving as committee members and reviewing this thesis.

I would like to thank Dr. Jianzhong Ruan for his encouragement and incredible help at each step throughout the term of my research. I would like to thank my friends Preethi, Anup, Sheela, Uday and Hindu for standing by me and supporting me during the tough times.

A special thanks to my parents for their unconditional love and support throughout my life. This thesis is dedicated to my sister **Ramya Kankanala** who has been my friend, guide and philosopher.

## TABLE OF CONTENTS

	Page
ABSTRACT.....	iii
ACKNOWLEDGEMENTS.....	iv
LIST OF FIGURES .....	vii
SECTION	
1. INTRODUCTION.....	1
2. METAL DEPOSITION SYSTEM OVERVIEW.....	3
3. RELATED WORK.....	5
4. MULTI-AXIS SLICING.....	8
4.1. SLICE AND TREE DATASTRUCTURE.....	8
4.2. MULTI- AXIS METAL DEPOSITION SYSTEM.....	12
4.3 DIRECT 3D LAYER FABRICATION.....	12
4.3.1. 3D layer.....	12
4.3.2. Direct 3D layer deposition technique.....	13
4.4. MULTI-AXIS SLICING METHOD.....	14
4.4.1. Analysis of topological information.....	14
4.4.2. Slicing direction change.....	16
4.4.3. The hierarchy graph structure.....	24
4.5. COLLISION CONTROL.....	25
4.5.1. Slicing algorithm.....	25
4.5.2. Slicing sequence.....	27
4.5.3. Distance-Angle method.....	30

5. INTEGRATION.....	35
5.1. ZIGZAG PATH PLANNING.....	35
5.2. THE TOOL-PATH DIRECTION DETERMINATION.....	35
5.3. GM CODE GENERATION.....	36
5.4. INTEGRATED PART.....	37
6. CONCLUSIONS.....	41
BIBLIOGRAPHY.....	43
VITA.....	47



## LIST OF FIGURES

Figure	Page
2.1. Basic system hardware required for metal forming system.....	4
3.1. Deposition system with and without support structure.....	5
3.2. Using transition wall fails to build cylinder overhang.....	7
4.1. Parallel slicing of spline.....	8
4.2. Adaptive slicing of spline .....	9
4.3. Slice class.....	10
4.4. Slice with and without outer wire .....	11
4.5. Tree structure depicting parent child relationship of wires.....	11
4.6. 3D layer illustration .....	13
4.7. A part built using direct 3D layer .....	14
4.8. The scenarios of upper and lower slice.....	15
4.9. Construction of splitting surface.....	17
4.10. Slicing direction searching.....	19
4.11. Code demonstrating change in layer thickness and slicing direction .....	20
4.12. Bearing seat example .....	22
4.13. Hierarchy graph storage structure .....	25
4.14. Building sequence for example in Figure 4.13 .....	25
4.15. Flowchart of the algorithm.....	26
4.16. Powder stream formed using a coaxial nozzle.....	28
4.17. Geometric model of the deposition tool.....	29
4.18. The collision check illustration.....	29
4.19. The distance angle of the deposition tool .....	30
4.20. Distance-Angle demonstration.....	31
4.21. Arch Model with all depositing sections .....	33
5.1. Bounding boxes with different ratios.....	35
5.2. Zigzag path illustration .....	36
5.3. GM code format.....	37
5.4. Original Spartan part.....	38

5.5. Zigzag at different levels on Spartan ..... 39

5.6. Zigzag illustration on Spartan ..... 40

## 1. INTRODUCTION

Layered Manufacturing (LM) technology has provided an efficient approach to build parts directly from a CAD model [1-5] since its appearance in mid 80s. Most of the current RP systems are built on a 2.5-D platform. Among them, the laser-based deposition process is a potential technique that can produce fully functional parts directly from a CAD system and eliminate the need for an intermediate step. As a result, the current laser deposition process, such as LENS (Laser Engineering Net Shaping [6]) from Optomec Inc., can only build fully dense metal with relatively simpler geometry [7,8]. In order to fabricate parts with overhang or complicated geometric shapes, support structures are commonly used. Such structures are not desirable for high strength and high temperature materials such as metals and ceramics since these support structures are very difficult to move.

Equipped with multi-axis capability, the direct laser deposition process can change the building direction as needed. With extra rotation freedoms, the support structures may not be necessary for the deposition process in order to build a complicated shape. Figure 3.1 illustrates the process to build an overhang structure on a 2.5-D and multi-axis deposition system. On the other hand, the systems become so complex that an automatic slicing planner is needed to drive such systems. The research on 2.5-D slicing has been performed widely and yielded many sound results. However, these results can be directly applied on the multi-axis slicing process since none of them deal with the change in building or slicing direction.

Presented here is a study on the multi-axis slicing based on the topological information of neighboring layers. This slicing method can change the building direction to eliminate or decrease the usage of a support structure. Integrated with an angle collision checking model, the building sequence can be determined. The research is organized as follows: 2.5D slicing methods and some research on multi-axis slicing are summarized and new ones are defined and analyzed. The topological analysis is discussed in next section. The collision checking model is also illustrated under slicing direction change. The multi-axis slicing procedure is presented in the next section. Some examples are shown and a discussion is presented in ahead.

## 2. METAL DEPOSITION SYSTEM OVERVIEW

Usually, a laser powder-based metal deposition process consists of a high power laser, powder delivery system, cladding nozzle, and motion control. In a typical laser powder-based metal deposition process, powder is injected into the melt pool and then solidified to form the geometry. Different than other rapid prototyping processes, there is overlap between each track. Some unmelted powder material during one track deposition is melted when the laser scans the neighboring area and this effect may cause the uneven layer height deposition. To investigate this effect, experiments have been run using different laser scanning patterns in the Laser Aided Manufacturing Process (LAMP) lab at Missouri University of Science and Technology (Missouri S&T). LAMP's process is a multi-axis hybrid manufacturing process which can directly produce functional parts with machining accuracy [14]. The diode laser in the LAMP lab is used in this research to achieve better energy efficiency.

The basic system hardware for a rapid metal forming process includes an energy delivery system (laser head, optics system), powder delivery apparatus (powder feeder, nozzle, carriage gas), and a Computer Numerical Control (CNC) table for x-y motion and z-axis vertical motion. The CNC table can have three-axis or multi-axis motion for enhanced flexibility that is needed in forming more complex parts [8]. Figure 2.1 shows the basic system hardware required for a metal forming system.

In addition to the basic hardware, a metal forming system also consists of control system hardware, a cooling system for the powder nozzle, and a base plate. A cooling system is used for the powder nozzle because it is exposed to a thermal load by scattered

and reflected laser radiation. A base plate is normally used as a substrate on which metal layers are deposited until a complete part is formed. The base plate is removed by machining or by dissolving with certain chemicals, leaving the finished metal part. Control system hardware includes sensors, CCD cameras, and a computer workstation. Online control is an integral part of a metal forming system. The typical rapid metal forming software architecture includes the modeling of a three dimensional CAD model in standard Stereolithography (STL) format, generation of layer representation of the object which is equal to the deposition thickness, and creation of CNC codes for the tool path that are understandable by the machine controller. The research used feature based parts representations which were sliced into planar layers. Fully dense metal parts were built in the vertical direction feature by feature and one layer at a time.

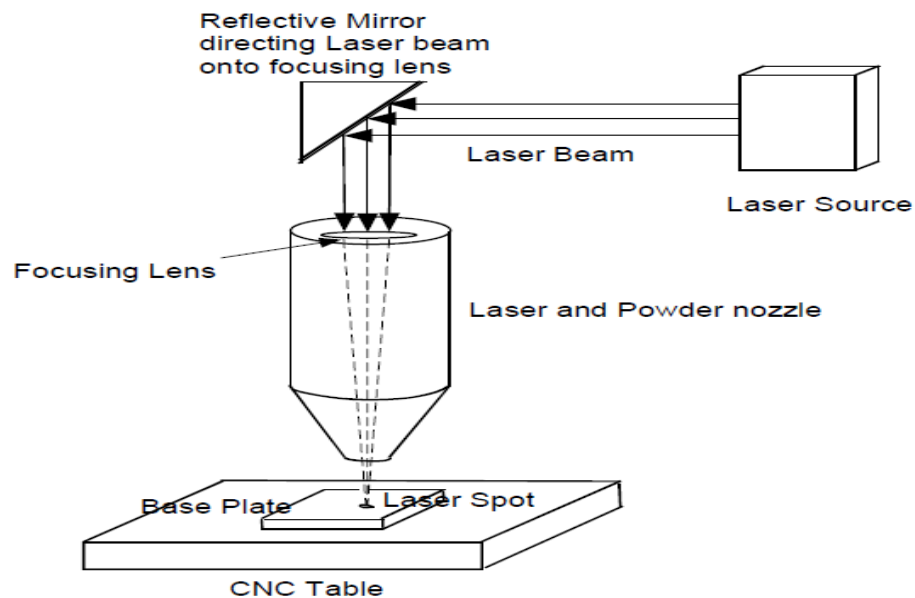


Figure 2.1. Basic system hardware required for a metal forming system

### 3. RELATED WORK

In LM processes, slicing is the process that is represented as a set of layers formed by "slicing" a CAD model with the set of horizontal planes [9]. The distance between planes is called "layer thickness". Difference in quality can be achieved by controlling the layer thickness. Research on 2.5-D slicing procedures and deposition tool-path.

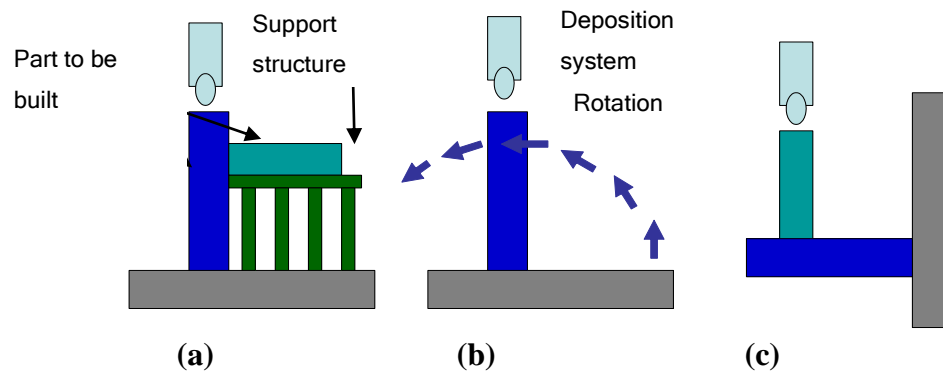


Figure 3.1. Deposition system with and without support structure (a) build part with support structure; (b) with multi-axis capability, after building the column, the table can be rotated: (c) After rotation. continue to build the component from another direction

for layered manufacturing processes has been widely conducted. Cusp height is introduced by Dolenc and Makela [10] to control the tolerance. Since then, various efficient and reliable processes for 2.5-D slicing procedures have been studied based on controlling cusp height and meeting the critical surfaces [11-14]. Some researchers presented a slicing method using volume difference between adjacent slicing layers [15, 16]. Rather than computing the cusp height, this method determines layer thickness by comparing the area difference between two neighboring layers after conducting Boolean

operations. To some extent, these methods help to improve the efficiency and quality for the deposition system. However, not all of these methods adopt multi-axis into the slicing algorithm. Thus, they lack the ability to handle a more complicated multi-axis layered manufacturing process.

Recently, some research has been focused on multi-axis slicing to drive the multi-axis deposition system in order to deliver a more efficient manufacturing system. The project method is reported to be used to find the new building direction for overhang structure [17]. In this work, the part is decomposed according to the projected information. The building direction is determined from a building map constructed for a decomposed component. However, in some cases, the building direction does not match the surface normal, which leads to a greater staircase effect. Furthermore, a collision may occur which is difficult to avoid. Figure 3.2 shows an example to illustrate this situation. Thin/transition wall can be used to build overhang structures on the platform of the multi-axis deposition process.

In this method, the building/slicing direction of one slice is determined by the previous layer. To build an overhang structure, the machine is turned  $90^\circ$  to start depositing a transition, named thin wall. After the wall is finished, the part is flipped back to its original direction to continue the deposition process. In this method, a so called 3D slicing to generate non-uniform thickness layers is used to slice the curve (freeform) surface. However, transition/thin wall usage is limited by physical capability and sometimes its results cannot be realized in the deposition system [18,19]. In some cases, the required rotation deposition is impossible to implement.



Figure 3.2 shows that limitation. It will benefit the multi-axis deposition process significantly to integrate projection and 3D slicing together and the obstacle is an automatic determination on how to apply different slicing methods. In other words, the challenge is to understand the geometry and use the information to automatically apply the different slicing strategies. A slicing method based on the analysis of topological information of neighboring layers is presented here.

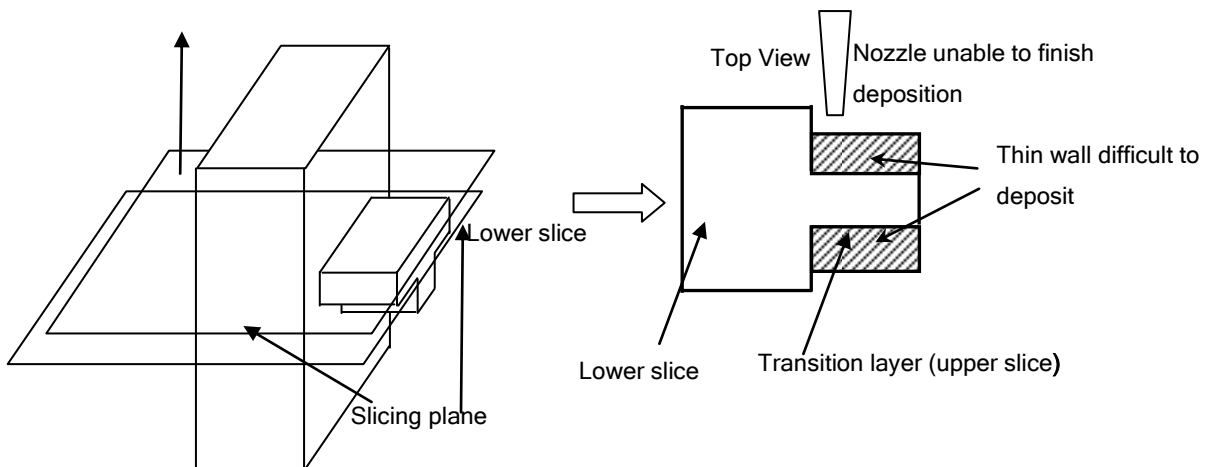


Figure 3.2. Using transition wall fails to build cylinder overhang

## 4. MULTI-AXIS SLICING

### 4.1. SLICE AND TREE DATASTRUCTURE

Slicing is cutting a CAD part with a plane. A plane is formed using a point and a direction. Slicing is necessary because every part is deposited layer by layer and not all at once. Every model is sliced according to its geometry. There exist two types of slicing, namely parallel slicing and adaptive slicing. Parallel slicing has uniform layer thickness. Every two layers are equidistant from each other. The slicing direction is parallel to its base throughout the part from bottom to the top.

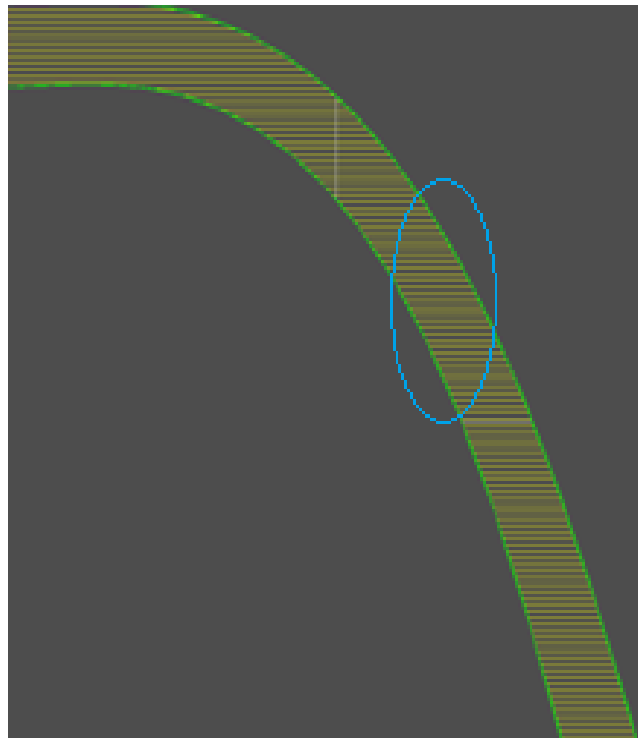


Figure 4.1. Parallel slicing of spline

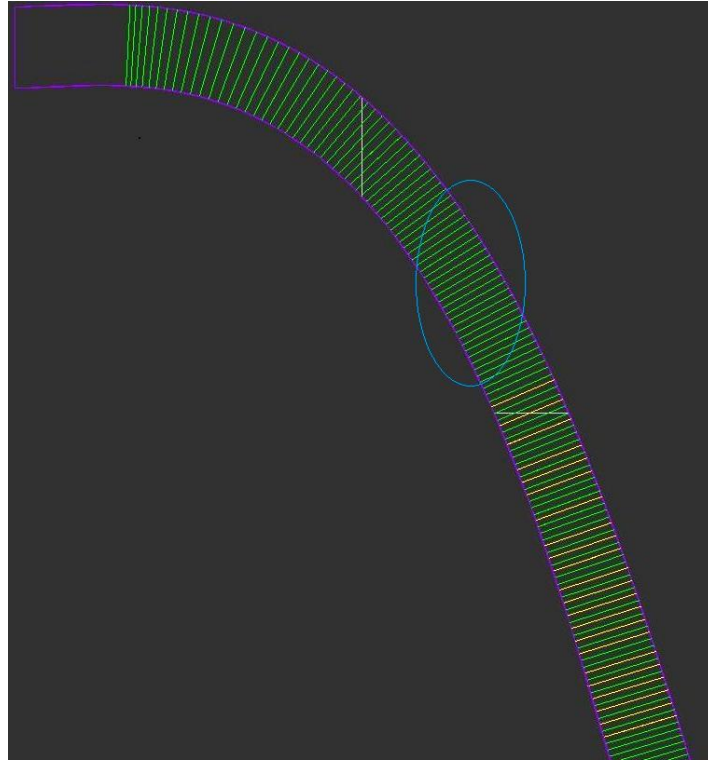


Figure 4.2. Adaptive slicing of spline

Adaptive slicing, varies not only layer thickness but also in slicing/building direction. Aware of potential problems of previous research on slicing, the work focuses on innovative geometry reasoning and analysis tool-centroidal axis. Similar to medial axis, it contains geometry and topological information but is significantly computationally cheaper. Using a centroidal axis as a guide, the multi-axis slicing procedure is able to generate a "3-D" layer or change slicing direction as needed automatically to build the part with better surface quality. Various examples to demonstrate the feasibility and advantages of centroidal axis and its usage in the multi-axis slicing process are presented here. Figures 4.1 and 4.2 show the difference between parallel and adaptive slicing.

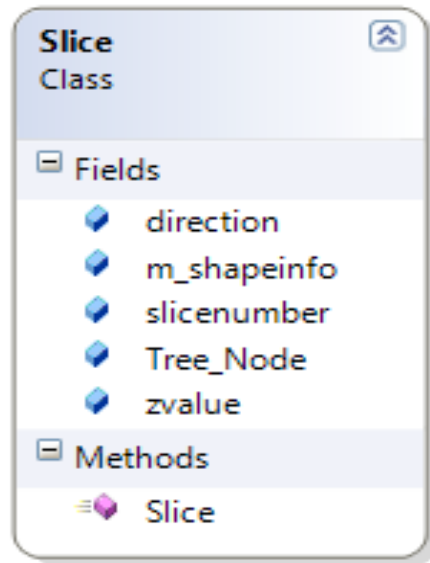


Figure 4.3. Slice class

Figure 4.3 discusses the slice class with the fields denoting the slice as a shape under `m_shapeinfo`, its slicing direction as `direction`. The slice number is the sequence of the slice starting from the first one. The `zvalue` is the height at which slicing was performed. `Tree_Node` is object of tree class. All the wires of a particular slice are arranged in a tree structure. Figure 4.4 (a) shows a slice with outer wire and inner wires and Fig 4.4 (b) shows one without outer wire. Though there is no outer wire, the inner wires are considered parents of its children. Figure 4.5 shows that the outer wire is denoted as a parent node and inner wires are denoted as children.

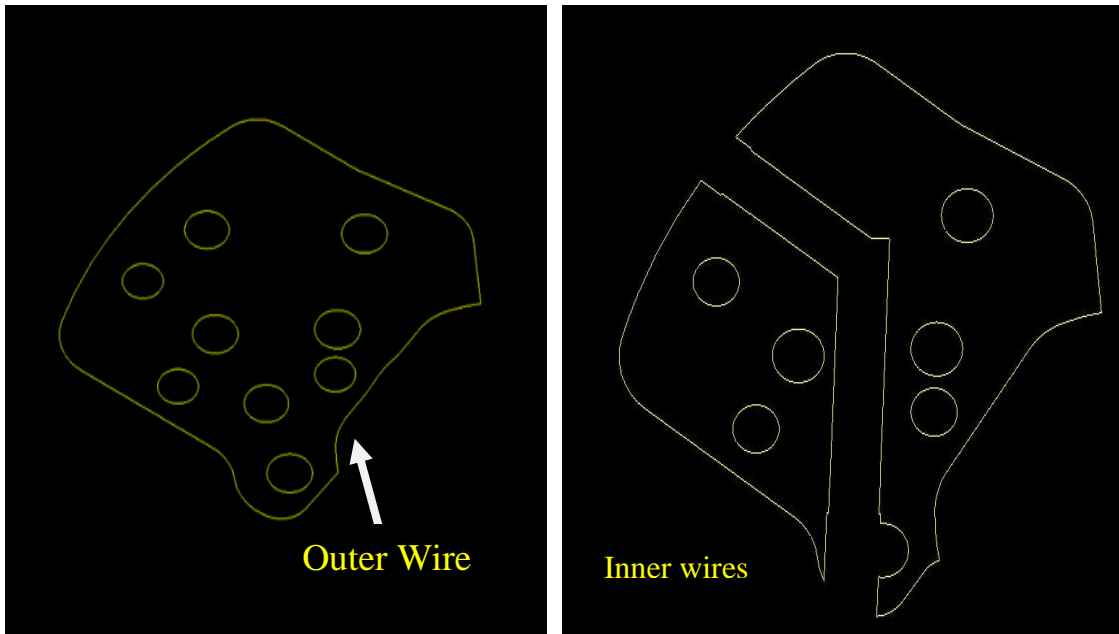


Figure 4.4. Slice with and without outerwire (a) A slice with outer wire (b) Without outer wire

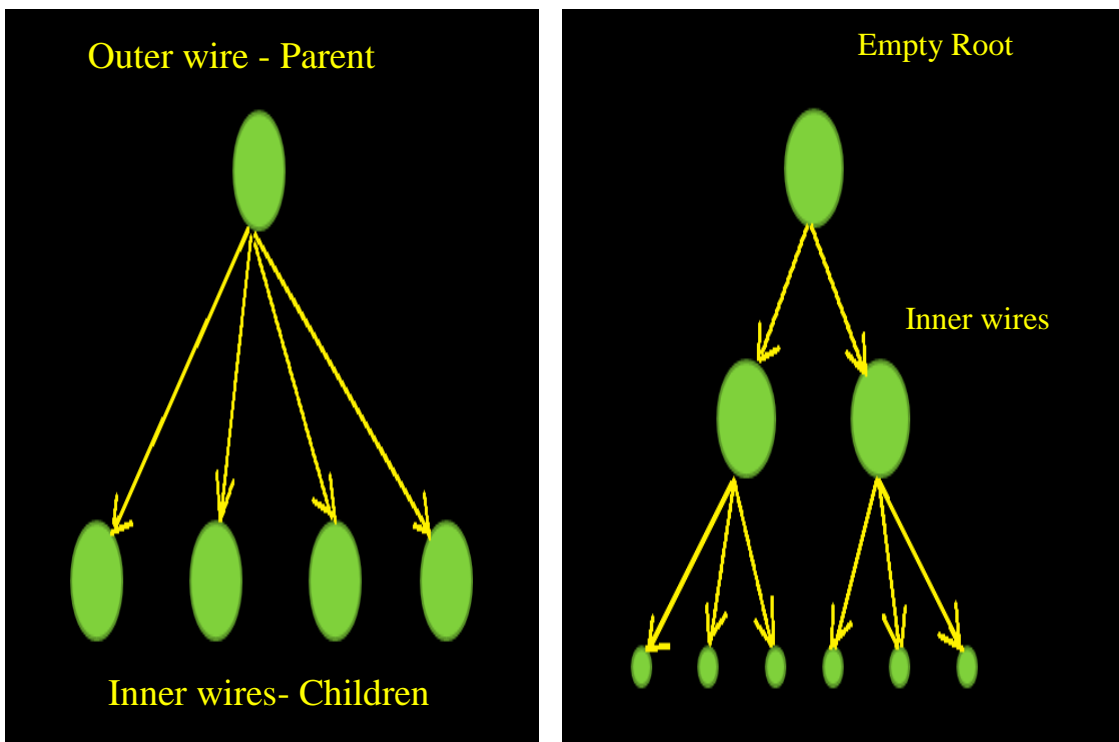


Figure 4.5. Tree structure depicting parent-child relationship of wires

## **4.2 MULTI-AXIS METAL DEPOSITION SYSTEM**

The Laser Aided Manufacturing Process (LAMP) at Missouri University of Science and Technology (Missouri S&T) has developed a multi-axis laser metal deposition which can directly deliver a part with machined accuracy from its CAD model. The system consists of a Fadal 3016L 5-axis CNC workstation, a 1.0 KW Coherent Inc, diode laser, a powder feeder from Bay State Surface Technologies (model 1200), a Cladding head from Precitec (model KG YC50), includes a coaxial nozzle and focusing lens. During deposition, the laser is focused to a small spot (approximately 2.5 mm in diameter) on the substrate by an optical system to achieve a high power density and forms a melt pool. The powder is heated while traveling through the laser beam and is injected into the melt pool where it is melted. When the laser moves away from the location, the melt pool solidifies. During this process, the laser interacts with the material (powder and substrate) and builds a shape.

## **4.3 DIRECT 3D LAYER FABRICATION**

**4.3.1. 3D layer.** The multi-axis slicing method presented is based on the geometric information of neighboring slicing layers and the slicing direction can vary with layers; thus, the slicing direction can be changed along a series of layers. As a result, a so called 3D layer can be produced as shown in Figure 4.6. The layer thickness of a typical slicing layer is uniform. However, in a 3D layer, the layer thickness is not uniform as the slicing plane may not be parallel to the previous slice anymore. By using 3D layer, multi-axis slicing method can be more efficient.

**4.3.2. Direct 3D layer deposition technique.** Fabrication of a 3D layer is a challenge to metal deposition processes. There are several different methods to produce a 3D layer, such as using hybrid manufacturing process [20] to machine a 3D layer, or using fuzz control [21] to vary the laser power based on camera sensor to deposit a 3D layer. Authors have studied a direct 3D layer deposition technique by changing the laser scanning speed [21]. In this method, an empirical model is presented to predict the layer height as a function of the laser scanning speed for a single track deposited near the substrate. Using this model, the toolpath for the 3D layer deposition and scanning speed profile are generated. Non-parallel toolpath generation allows the deposition to follow the geometry of a part more precisely, when compared to parallel layer deposition. Direct 3D layer deposition is beneficial to multi-axis slicing/deposition. Using the direct 3D layer deposition technique enables freeform parts to be fabricated more accurately and more efficiently by eliminating the staircase effect and shortening the deposition time. Figure 4.7 shows an example fabricated by using the direct 3D layer deposition technique.

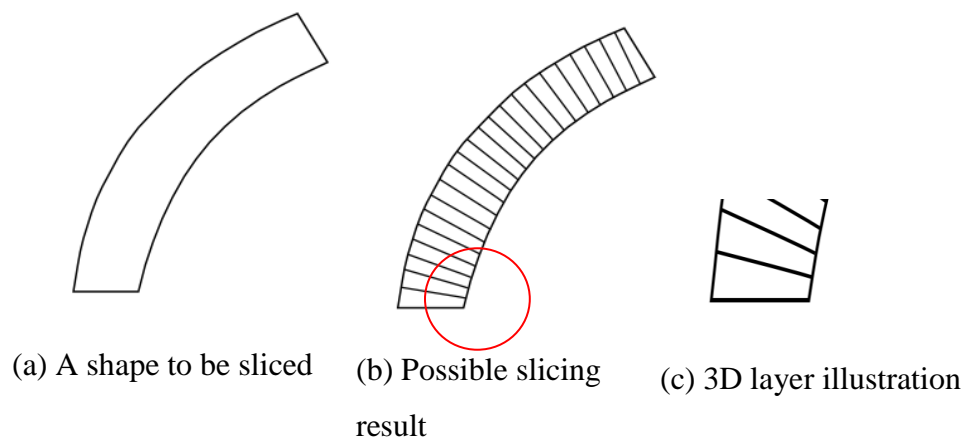


Figure 4.6. 3D layer illustration



Figure 4.7. A part built using direct 3D layer

#### 4.4. THE MULTI-AXIS SLICING METHOD

**4.4.1. Analysis of topological information.** As stated in the earlier section, the 3D slicing method presented uses the topological relationship between neighboring slices. As shown in Figure 4.8, the projection results of two neighboring slices can generally be put into three different scenarios, defined below. The scenario in Figure 4.8(a) indicates that the two slices are not related to each other. The scenario in Figure 4.8(b) indicates that two slices can have same slicing direction. The scenario in Figure 4.8(c) can be further analyzed.



$$A_{upper} - (A_{upper} \cap A_{lower}) = \begin{cases} A_{upper} \\ \phi \\ \Delta A_1, \Delta A_2, \dots, \Delta A_n; \sum_{i=1}^n \Delta A_i < A_{upper} \end{cases} \quad (1)$$

A centroid can be identified for each overhang shape, such as  $A_1, A_2$  in Figure 4.8(c). Assuming that  $\vec{C}_b$  is the centroid of the slicing surface at the bottom layer and the  $\vec{C}_i$  is the centroid of the  $i^{\text{th}}$  shape illustrated in Figure 4.7(c). Unit vector  $\vec{N}_b$  is the normal

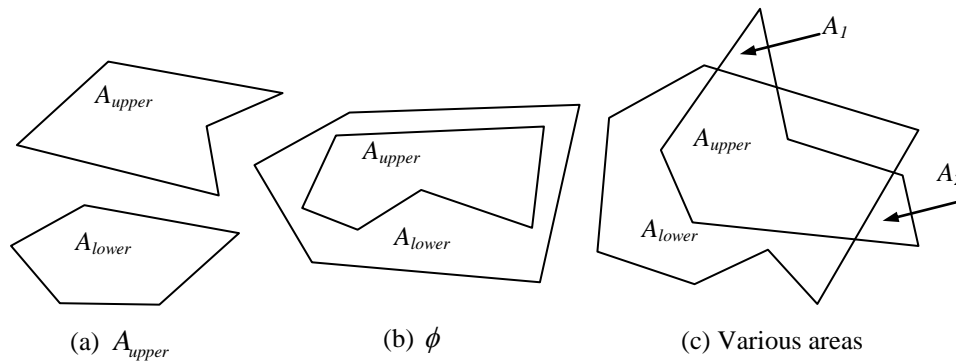


Figure 4.8. The scenarios of upper and lower slice  $A_{upper} - A_{lower}$

vector of the bottom layer. Let  $\vec{P}_{b(i)}$  be the point on the bottom layer which is closest to  $\vec{C}_i$ , then a vector can be formed by

$$\vec{V}_i = \vec{C}_i - \vec{P}_{b(i)} \quad (2)$$

The angle between  $\vec{V}_i$  and  $\vec{N}_i$  can be obtained, denoted as  $Ang_i$ . Such an angle is used to determine the change in slicing direction. If  $Ang_i$  is greater than a pre-defined value  $\alpha$ , then the search for new slicing direction is performed. If  $Ang_i$  is greater than another pre-defined value  $\beta$  ( $\beta > \alpha$ ), the slicing direction is rotated  $90^\circ$  from the normal of the bottom layer.

**4.4.2. Slicing direction change.** When  $Ang_i$  is greater than another pre-defined value  $\beta$ , the slicing direction is rotated  $90^\circ$  from the normal of the bottom layer toward  $\vec{C}_i$ . A split plane is needed to separate the part. In this research, the project result is used to identify the plane. Shown in Figure 4.9, the boundary line can be extracted using the projection result. The boundary line can be approximated by N points ( $\vec{S}_{b(1)}, \vec{S}_{b(2)}, \dots, \vec{S}_{b(N)}$ ). A bounding box can be computed for these points. The center of the bounding box is selected as the point to perform the splitting. In cases, where no bounding box can be found (a straight line), the middle point of boundary line is chosen.

The normal direction of the split plane is given by

$$\vec{N}_{st} = \vec{N}_b \times (\vec{V}_i \times \vec{N}_b) \quad (3)$$

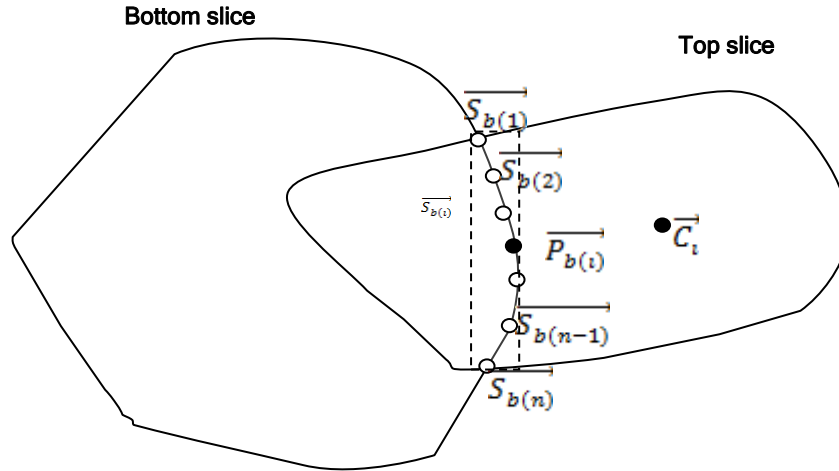


Figure 4.9. Construction of splitting surface

When  $\alpha < \text{Ang}_i < \beta$ , it indicates that a slight slicing direction change is needed. As stated in the earlier section that 3D slicing is used instead of uniform slicing.  $\vec{C}_b$  is the centroid of the slicing surface at the bottom layer and unit vector  $\vec{N}_b$  is the real normal vector of the bottom layer. The value  $h_{\max}$  is the maximum height for each deposition layer.  $\vec{C}_t$  is the centroid of the top layer obtained.

The algorithm starts with the prediction step. Point  $\vec{G}_t$  is a guessed point for the next layer given by

$$\vec{G}_t = \vec{C}_b + h_{\max} * \vec{N}_b \quad (4)$$

The slicing direction is given by

$$\vec{D}_i = \vec{C}_i - \vec{C}_b \quad (5)$$

It is obvious that  $h^*$  is greater than  $h_{\max}$ , which is not acceptable for metal deposition process for a single layer slice. The layer height is shift down by

$$y = \left[ \frac{h}{h^*} \right] y^* \quad (6)$$

where  $y$  is the next height,  $y^*$  is the current height.

The process is repeated until the  $h^*$  is less than  $h_{\max}$  and  $Ang_i$  is less than  $\alpha$ .

The process mentioned above is clearly explained in Figure 4.10.

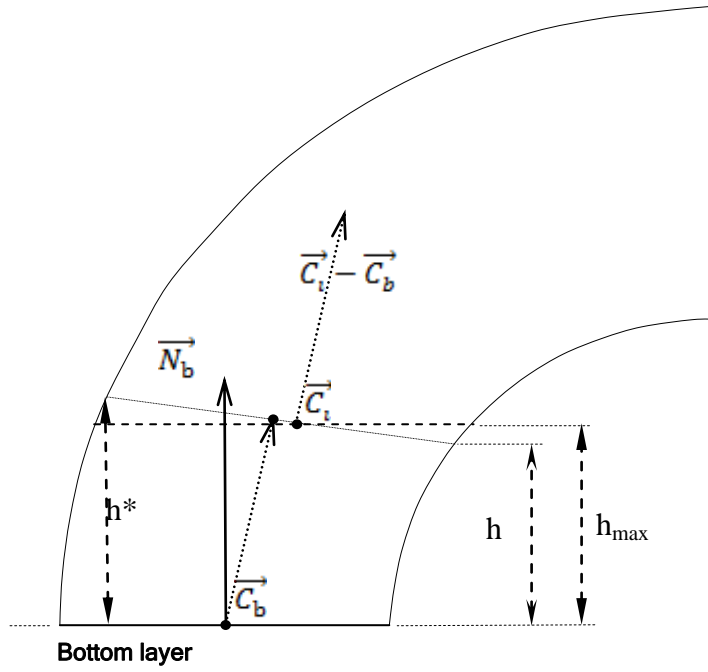


Figure 4.10. Slicing direction searching

```

//for determining layer thickness and slicing direction]

Standard_Real MLT=0.5; //layer thickness
gp_Vec Vector1;gp_Pnt Point1;
if((Delarea==ar1)|| (Delarea==ar2)||dst<50) //This is a fixed number
{
    cout<<"\n\n CHANGE IN SLICING DIRECTION IS NOT REQUIRED";
    Vector1=Vector;
    Point1=Point;
}
else
{
    cout<<"\n\n CHANGE IS REQUIRED";
    gp_Vec gv;
    gv.SetCoord((P5.X()-P4.X()), (P5.Y()-P4.Y()), P5.Z()-P4.Z()); //new direction
    Vector1=gv;

}

Point1=P4+ MLT*Vector1.Magnitude(); //new guessed point
gp_Pln gp(Point1,Vector1); //P5 //new Plane with guessed point and new direction
BRepAlgo_Section Sa(Sp,gp,Standard_True);
Sa.ComputePCurveOn1(Standard_True);
Sa.Approximation(Standard_True);
Sa.Build();
Ra = Sa.Shape(); //slice obtained after slicing with new plane
Bnd_Box bnds; //finds bounds of new slice
BRepBndLib::Add(Ra, bnds);
bnds.SetGap(1);
Standard_Real x1,y1,z1,x2,y2,z2;
bnds.Get(x1,y1,z1,x2,y2,z2);

bounds.Get(XMin, YMin, ZMin, XMax, YMax, ZMax); //find bounds for lower slice
gp_Pnt PF,PV,PF1,PV1;
PF.SetX(x1);PF.SetY(y1);PF.SetZ(z1);
PV.SetX(x2);PV.SetY(y2);PV.SetZ(z2);
PF1.SetX(XMin);PF1.SetY(YMin);PF1.SetZ(ZMin);
PV1.SetX(XMax);PV1.SetY(YMax);PV1.SetZ(ZMax);
Standard_Real len1,len2,len3,len4,Maxlen,Minlen;
len1=PF.Distance(PF1);
len2=PV.Distance(PV1);
len3=PF.Distance(PV);
len4=PF.Distance(PV1);

```

Figure 4.11. Code demonstrating change in layer thickness and slicing direction

```

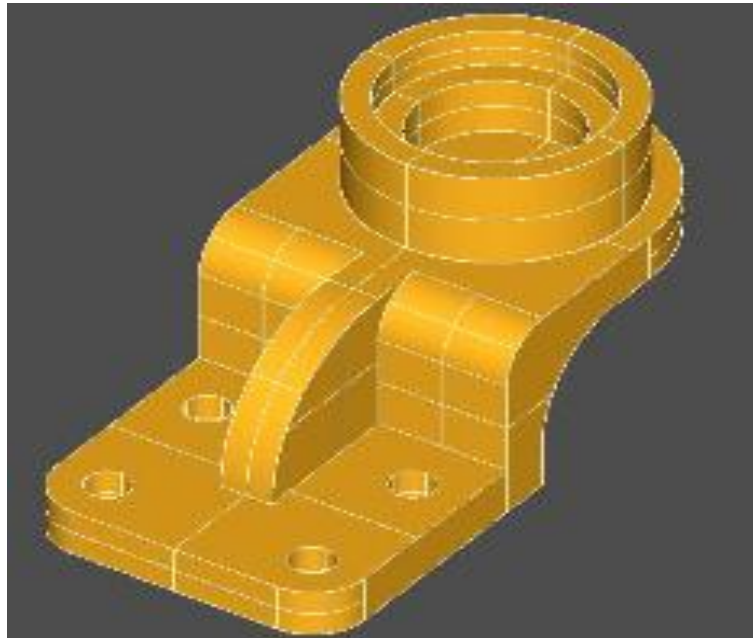
Maxlen=len1;Minlen=len1;
if(len2>Maxlen) //find Maxlen between 2 slices
{
    Maxlen=len2;
    if(len3>Maxlen)
    {
        Maxlen=len3;
        if(len4>Maxlen)
            Maxlen=len4;
    }
}

if(len2<Minlen) //find Minlen between 2 slices
{
    Minlen=len2;
    if(len3<Minlen)
    {
        Mainlen=len3;
        if(len4<Minlen)
            Minlen=len4;
    }
}

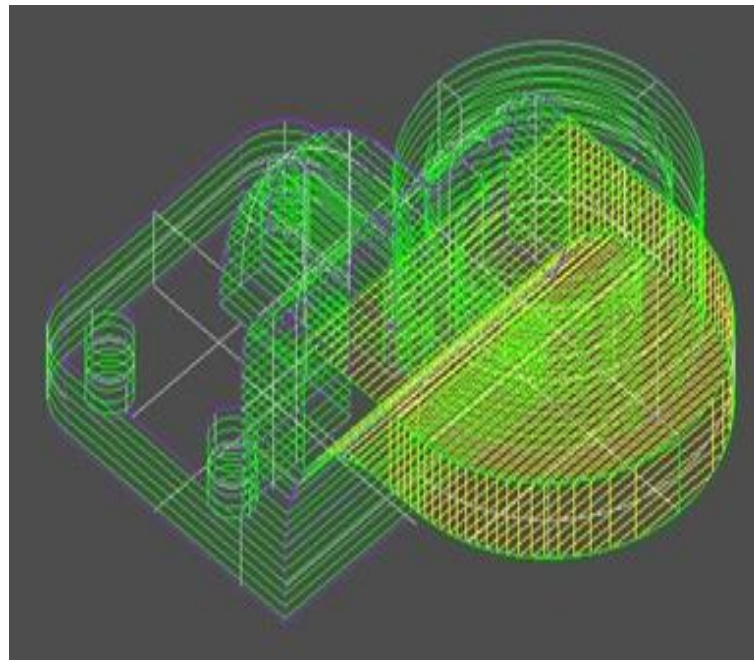
while(Maxlen>MLT) //If maximum distance between slices is greater than layer thickness
{
    Standard_Real z=Point1.Z()*(Minlen/Maxlen); //Adjust the height accordingly
    Point1.SetZ(z);
}

```

Figure 4.11. Continued



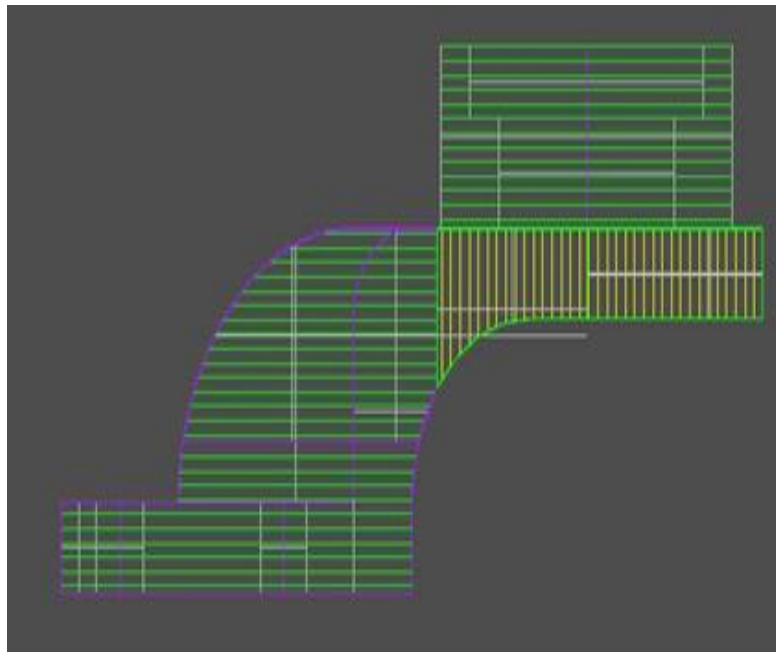
(a) Bearing seat



(b) The slicing result

Figure 4.12. Bearing seat example





(c) Side view of the slicing result

Figure 4.12. Continued

Figure 4.12 shows the slicing result of a bearing seat example. It demonstrates the split surface construction. The slicing direction is changed correspondingly. All slicing directions are shown in the Figure 4.12. First, the slicing direction is Z up (from the bottom to the top) and then a slicing direction change is identified. The direction is rotated  $90^\circ$  in order to build the overhang. The last portion of the part is constructed along Z up direction again.

**4.4.3. The hierarchy graph structure.** In order to organize all slices, a hierarchy graph structure is constructed. In this structure, multiple parents and children relationship is implemented to represent the topological relationship among slices layers. Each node in the structure represents a slicing layer. The graph formed from top to bottom follows the slicing sequence and slicing direction change. Shown in Figure 4.13, the slice A is the parent of slice C; slice C and slice D are both parents of slice E. Different from a tree structure, a child can have multiple parents. In a regular graph structure, the links between nodes are bi-directional.

However, the parent-children relationship is uni-directional in the hierarchy graph structures, which brings the following advantages:

- The slicing sequence among layers is clearly defined
- The hierarchy structure reduces the amount of the collision check, which is discussed later.
- The key slices (usually with multiple parents or children) in the hierarchy structure can be used to check the deposition quality

## 4.5. COLLISION CONTROL

**4.5.1. Slicing algorithm.** The entire multi-axis algorithm is developed based on analysis of topological information between neighboring layers. The slicing correction method is adopted to determine the slicing location and direction to meet the layer thickness and overhang angle requirement. The slicing sequence determination based on collision check is studied. The algorithm is listed in Figure 4.15.

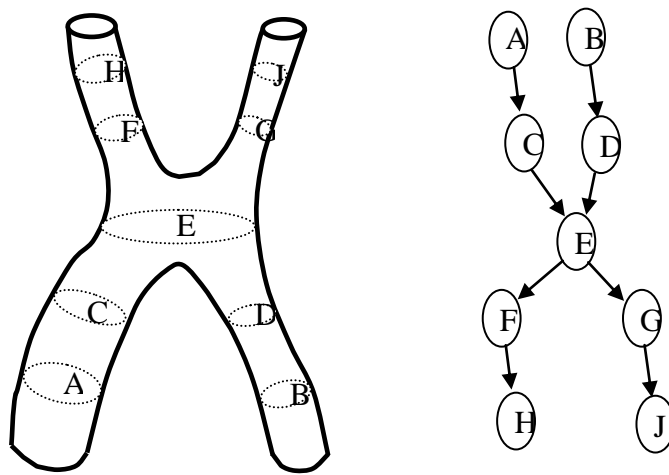
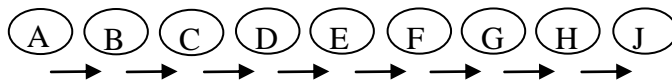
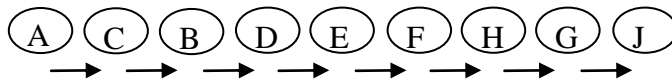


Figure 4.13. Hierarchy graph structure storage



(a) Building sequence without collision check



(b) Building sequence with collision check

Figure 4.14. Building sequence for example in Figure 4.13

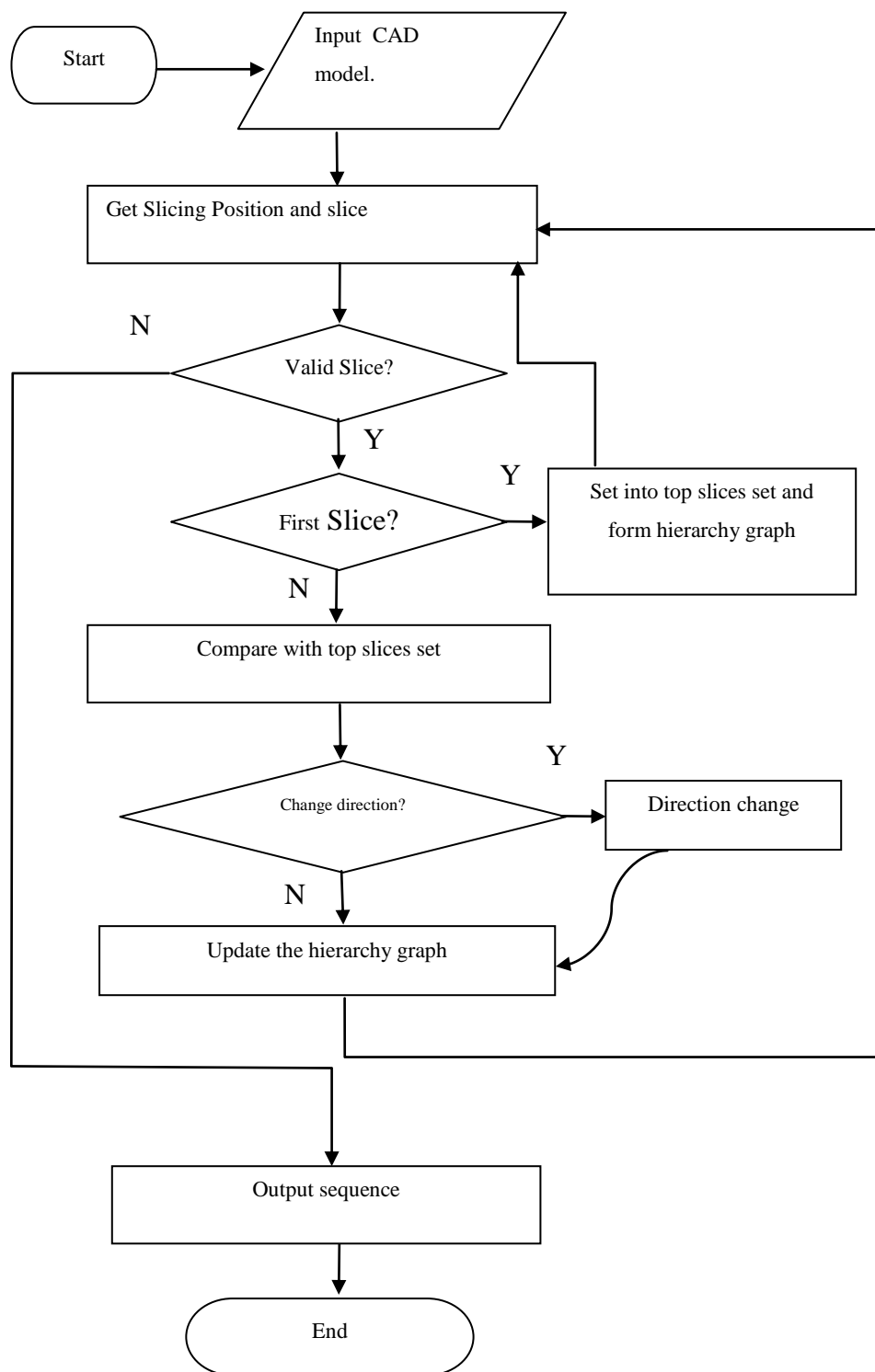


Figure 4.15. Flowchart of the algorithm

**4.5.2. Slicing sequence.** Usually, the cladding nozzle of a typical laser metal deposition process is coaxial or close to such a shape. The powder fed using this type of nozzles forms a stream which is in the shape of a cone shape, as shown in Figure 4.16. The nozzle and power stream shape can be simplified as a cone, illustrated in Figure 4.17. During the deposition process, no collision should occur.

$$B_{nozzle} \cap B_{deposit} = \emptyset \quad (7)$$

Where  $B_{nozzle}$  is the cone shape of nozzle and powder stream,  $B_{deposit}$  is the shape already deposited.

Since the deposition process uses slices to represent the geometry, such a constraint can be translated as when depositing a slice, no collision should occur between the  $B_{nozzle}$  and other slices. It should be noted that the deposition process is a material additive process and the geometry is “continuously growing” until the fabrication is finished; thus, the child layer does not collide with its parent layer. The collision check problem between geometry becomes the collision check between slicing layers. In other words, the deposition of a slice should not collide with the deposition of other undeposited slices.

Let  $S_1$  be the slice to be deposited and  $S_2$  is one of un-deposited slices, and  $\vec{N}_1, \vec{N}_2$  are their slicing directions (normal) respectively.

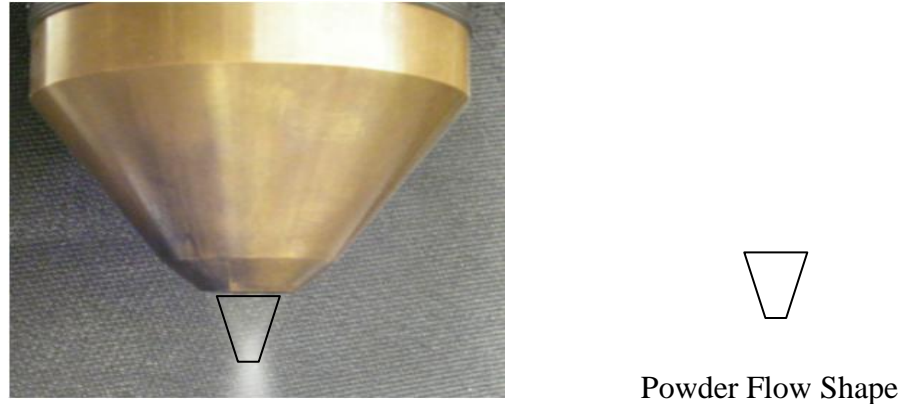
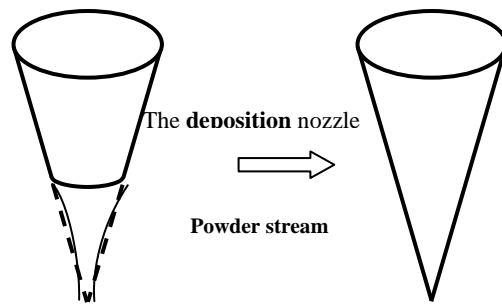


Figure 4.16. Powder stream formed using a coaxial nozzle

Then if one of conditions is met, the slice  $S_1$  can be deposited without preventing the deposition of slice  $S_2$ :

1. If  $S_2$  is a child of  $S_1$  or one of  $S_1$ 's leaves, then  $S_1$  can be deposited.
2. Since a slice is a plane, it separates the space into two half spaces. Let the top half space be the one above a slice and the bottom space is the other half space below the slice. If the entire  $S_2$  is in the top half space of  $S_1$ , then  $S_1$  can be deposited.
3. If the projection of  $S_1$  along  $-\vec{N}_2$  does not overlap with  $S_2$ , find a pair of points on  $S_2$  and  $S_1$  respectively ( $\vec{P}_2$  on  $S_2$  and  $\vec{P}_1$  on  $S_1$ ). If angle between  $\vec{P}_2\vec{P}_1$  and  $\vec{N}_2$  is greater than  $\theta/2$ , then  $S_1$  can be deposited, illustrated in Figure 4.18.



(a) The deposition nozzle and powder stream

(b) The simplified cone shape

Figure 4.17. Geometric model of the deposition tool used to find the deposition visibility map

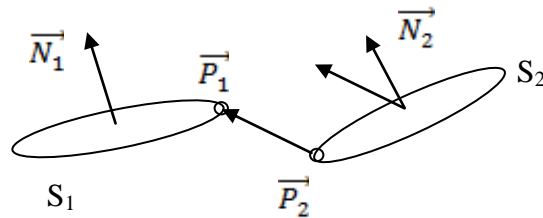


Figure 4.18. The collision check illustration

When all slices are generated, the other issue is to put slices in a collision-free sequence. With the collision check discussed above, the “jump” between slices can be minimized. It is straightforward that the nozzle should maintain its location except raising-up of the nozzle to next layers until the collision forces the nozzle to move to other locations. Figure 4.14 shows two different building sequences for the example shown in Figure 4.13.

**4.5.3. Distance-Angle Method.** In case of CAD models like Arch where the slicing starts from more than one base, the slicing mechanism changes a little. Here, the Distance angle algorithm is introduced. Distance angle algorithm considers the distance and angle criterion in order to divide the whole part into collision and collision free sections.

The presented algorithm has been implemented in VC++ using OpenCascade geometry kernel. Figure 4.19 and Figure 4.20 show the distance angle relationship used in the deposition of the arch model. When two slices are checked for distance and angle, the distance checked is the projected distance onto the height. The angle being checked is tool half angle. The angle between slices should always be greater than the tool half angle and the distance between the slices should always be greater than the projected distance.

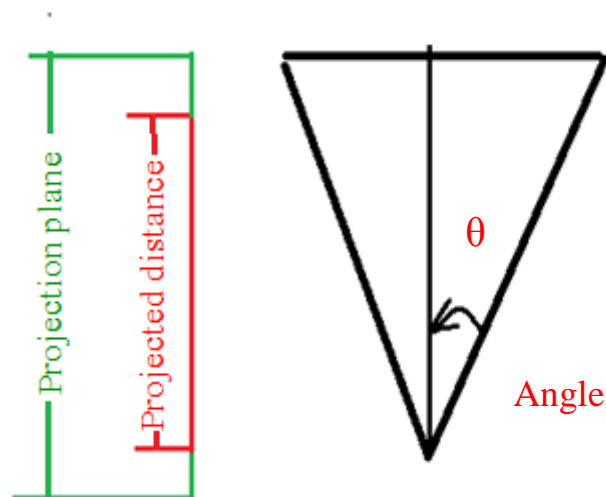


Figure 4.19. The distance angle of the deposition tool



Figure 4.21 shows an arch example with collision check. Figure 4.21 (b)-(e) shows the different sections in the sequence. In building process, the slicing algorithm puts the section 1 as the first section to be fabricated and the rest sections follow the sequence as shown in Figure 4.21. This example demonstrates the slicing direction slight change adjustment and the usage of hierarchy graph structure. The sections in same color represent non colliding sections. Sections in different colors are colliding sections. They cannot be deposited unless the lower similar colored sections are deposited.

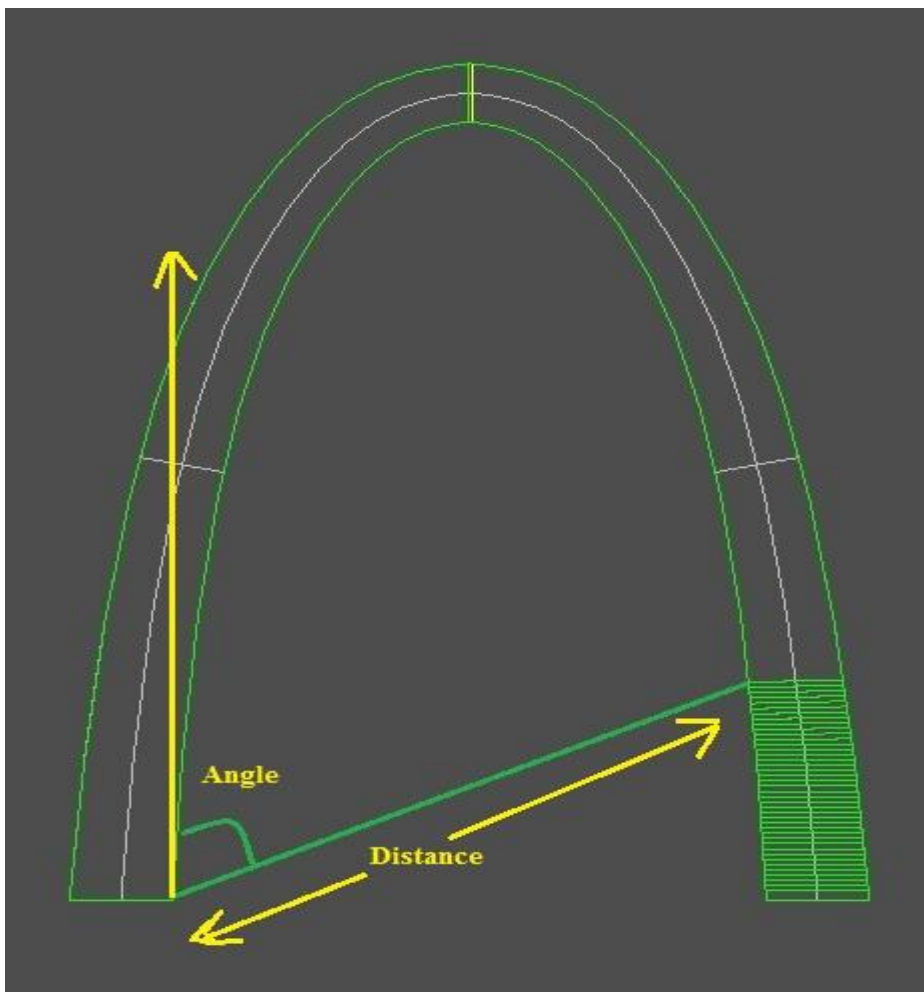
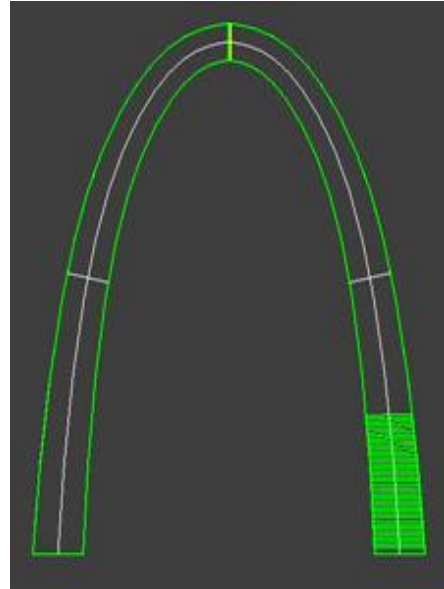


Figure 4.20. Distance-Angle demonstration

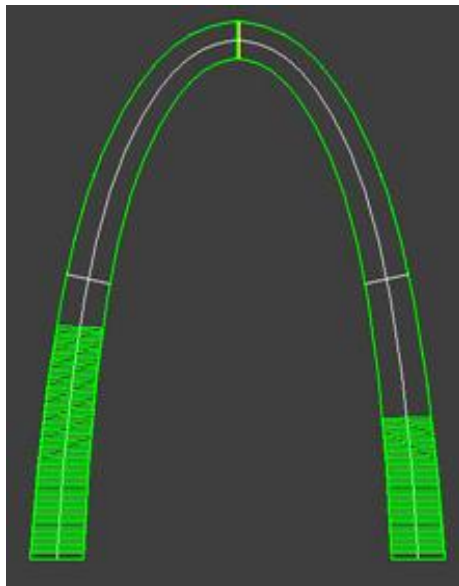
As shown in Figure 4.20 the first slice on the left is constantly being checked with the slices on the right for distance and angle. When the distance becomes smaller than the predefined distance value or the angle measures smaller than the tool half-angle the slicing is stopped. The slices registered so far as collision free are categorized as a section. There is a slicing switch to the other side for generating collision free sections since no more deposition can be performed on the same side. Now the topmost slice of the last section is the reference slice and algorithm is continued similarly till the top sections meet.



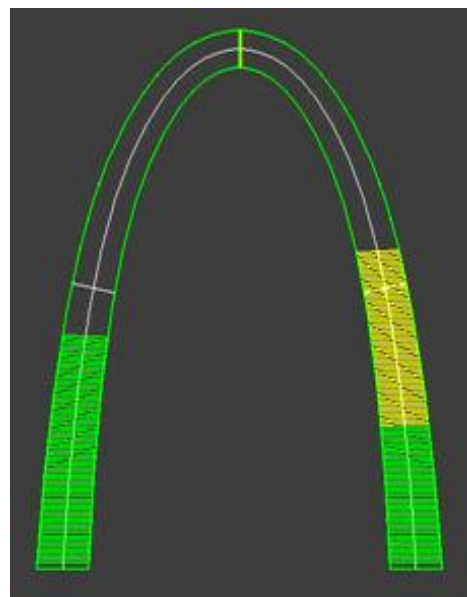
(a) Arch Model



(b) Section one

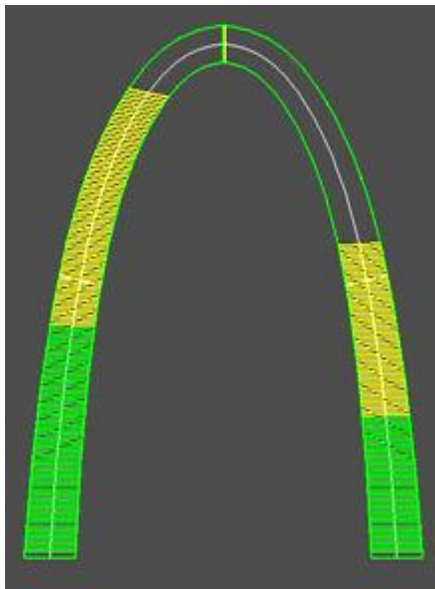


(c) Section two

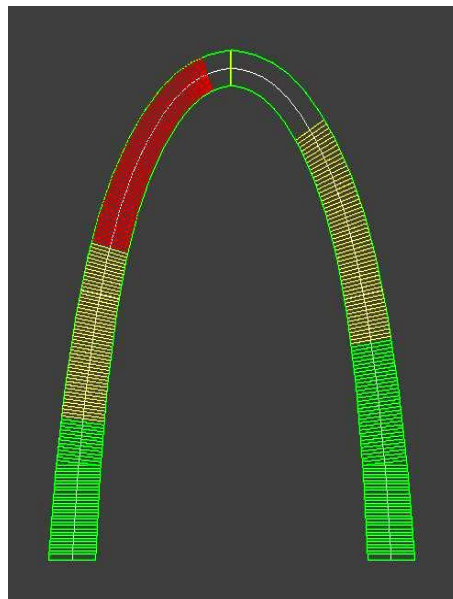


(d) Section three

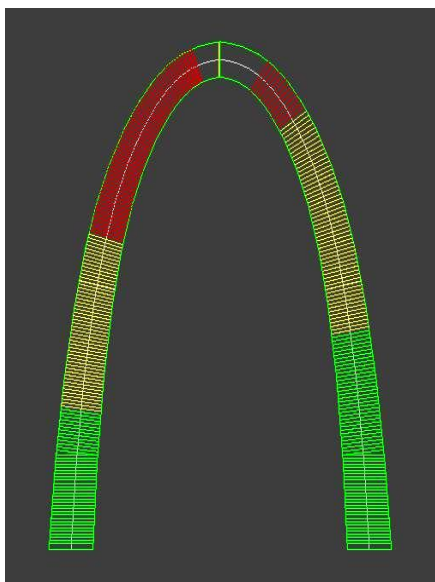
Figure 4.21. Arch Model with all depositing sections



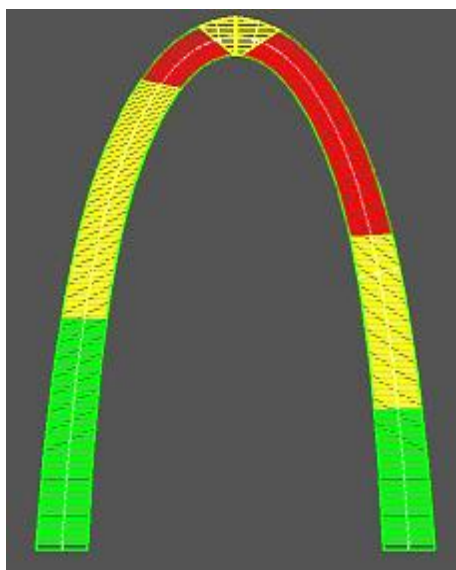
(e) Section four



(e) Section five



(g) Section six



(h) All Sections

Figure 4.21. Continued

## 5. INTEGRATION

### 5.1. ZIGZAG PATH PLANNING

A typical zigzag path consists of a number of parallel segments. The path travel direction and connection determines the efficiency. Path orientation determines the entire path length. In laser deposition process, the “idle” or non-working path should be as short as possible due to the energy consumption and potential material waste. Path connection determines the length of “idle” paths; thus, the tool-path orientation and path connection are two critical techniques in generating zigzag path.

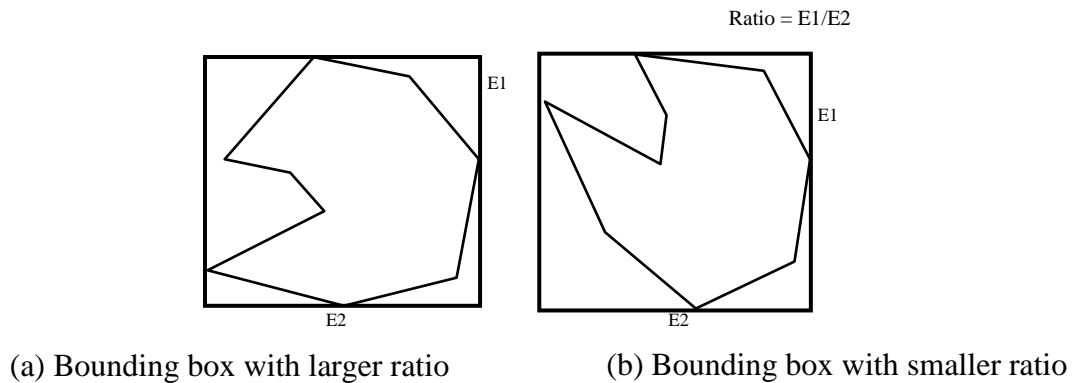


Figure 5.1. Bounding boxes with different ratios

### 5.2. THE TOOL-PATH DIRECTION DETERMINATION

In determining the tool-path direction, the bounding box concept is used to select the inclination direction for zigzag path instead of using the longest edge of a 2-D shape. The ratio of the longer edge to shorter edge of the bounding box is different, as shown in

Figure 5.1 and it is used to determine the inclination direction. According to Figure 5.1, the bounding box with the largest ratio is used to generate zigzag path. In order to find the bounding box with the largest ratio for a 2-D shape, the shape is rotated and the bounding box at each orientation is obtained.

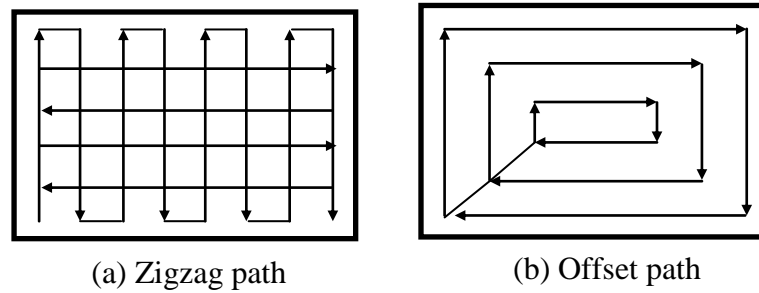
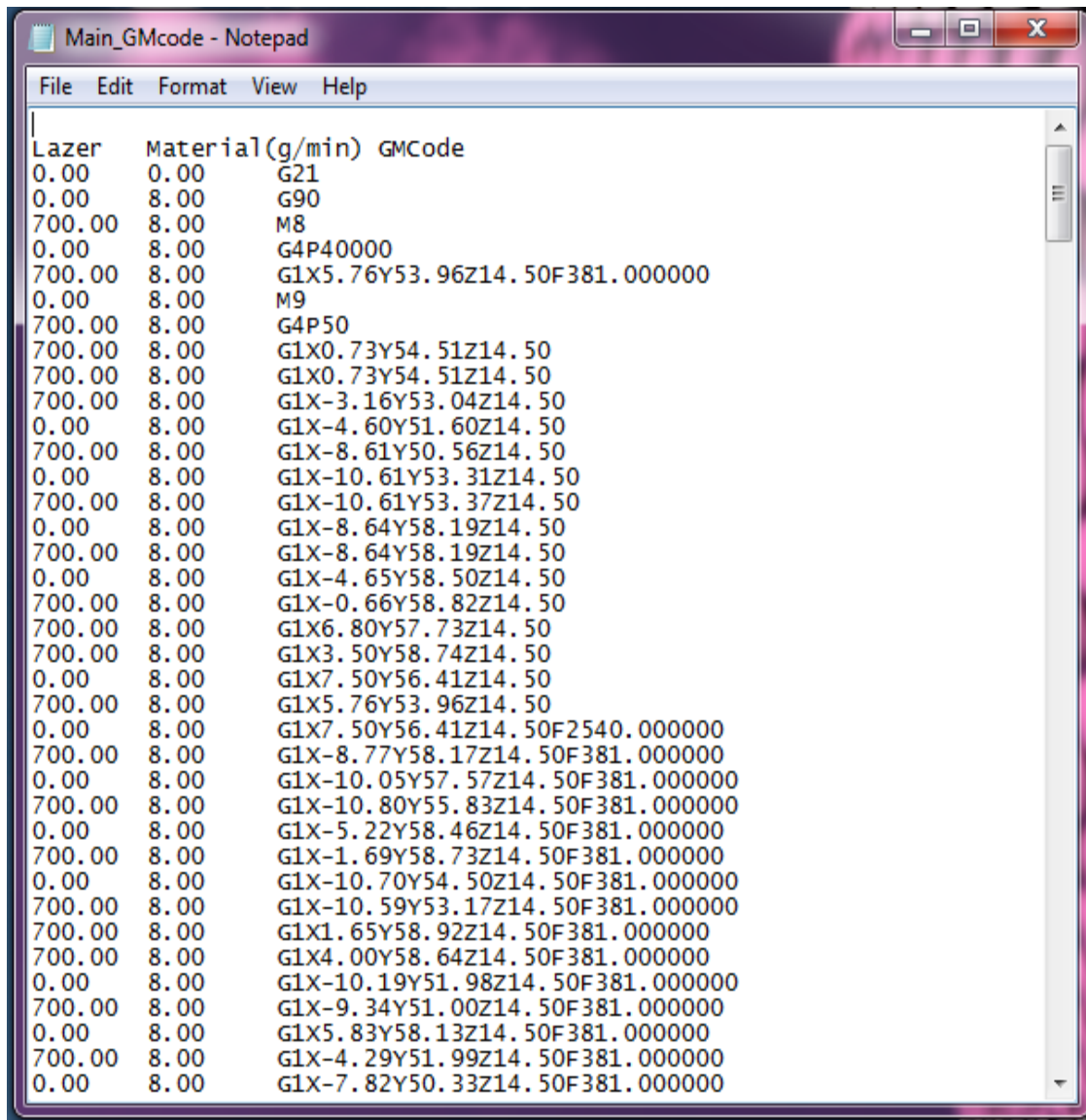


Figure 5.2. Zigzag and offset path

### 5.3. GM CODE GENERATION

GM Code is machine understandable format of a geometry and its depositing paths. The wires and the zigzag depositing path are represented using the points on it. All the points are documented in a text document. The figure shows below how to represent laser, powder feed-rate and the points depicting the deposition path. It is designed such that whenever a new wire or its zigzag path is encountered it writes down all the depositing points into a file with M8s and M9s are placed accordingly during run-time. The first column is about the laser power on/off. It is 0.00 when off and 700.00 when on. Column two is about powder material feed-rate. It is 0.00 when off and 8.00 when on. The code has points with X, Y and Z coordinates to be deposited.



```

Main_GMcode - Notepad
File Edit Format View Help
Lazer Material(g/min) GMCode
0.00 0.00 G21
0.00 8.00 G90
700.00 8.00 M8
0.00 8.00 G4P40000
700.00 8.00 G1X5.76Y53.96Z14.50F381.000000
0.00 8.00 M9
700.00 8.00 G4P50
700.00 8.00 G1X0.73Y54.51Z14.50
700.00 8.00 G1X0.73Y54.51Z14.50
700.00 8.00 G1X-3.16Y53.04Z14.50
0.00 8.00 G1X-4.60Y51.60Z14.50
700.00 8.00 G1X-8.61Y50.56Z14.50
0.00 8.00 G1X-10.61Y53.31Z14.50
700.00 8.00 G1X-10.61Y53.37Z14.50
0.00 8.00 G1X-8.64Y58.19Z14.50
700.00 8.00 G1X-8.64Y58.19Z14.50
0.00 8.00 G1X-4.65Y58.50Z14.50
700.00 8.00 G1X-0.66Y58.82Z14.50
700.00 8.00 G1X6.80Y57.73Z14.50
700.00 8.00 G1X3.50Y58.74Z14.50
0.00 8.00 G1X7.50Y56.41Z14.50
700.00 8.00 G1X5.76Y53.96Z14.50
0.00 8.00 G1X7.50Y56.41Z14.50F2540.000000
700.00 8.00 G1X-8.77Y58.17Z14.50F381.000000
0.00 8.00 G1X-10.05Y57.57Z14.50F381.000000
700.00 8.00 G1X-10.80Y55.83Z14.50F381.000000
0.00 8.00 G1X-5.22Y58.46Z14.50F381.000000
700.00 8.00 G1X-1.69Y58.73Z14.50F381.000000
0.00 8.00 G1X-10.70Y54.50Z14.50F381.000000
700.00 8.00 G1X-10.59Y53.17Z14.50F381.000000
700.00 8.00 G1X1.65Y58.92Z14.50F381.000000
700.00 8.00 G1X4.00Y58.64Z14.50F381.000000
0.00 8.00 G1X-10.19Y51.98Z14.50F381.000000
700.00 8.00 G1X-9.34Y51.00Z14.50F381.000000
0.00 8.00 G1X5.83Y58.13Z14.50F381.000000
700.00 8.00 G1X-4.29Y51.99Z14.50F381.000000
0.00 8.00 G1X-7.82Y50.33Z14.50F381.000000

```

Figure 5.3. GM code format

#### 5.4. INTEGRATED PART

A given CAD model is sliced using multi-axis slicing and slices are obtained at each level. A slice is then categorized into wires. The zigzag method is used to for obtaining depositing paths in a 2D plane. Figures 5.5 (a) and (b) show the depositing paths obtained by the zigzag process

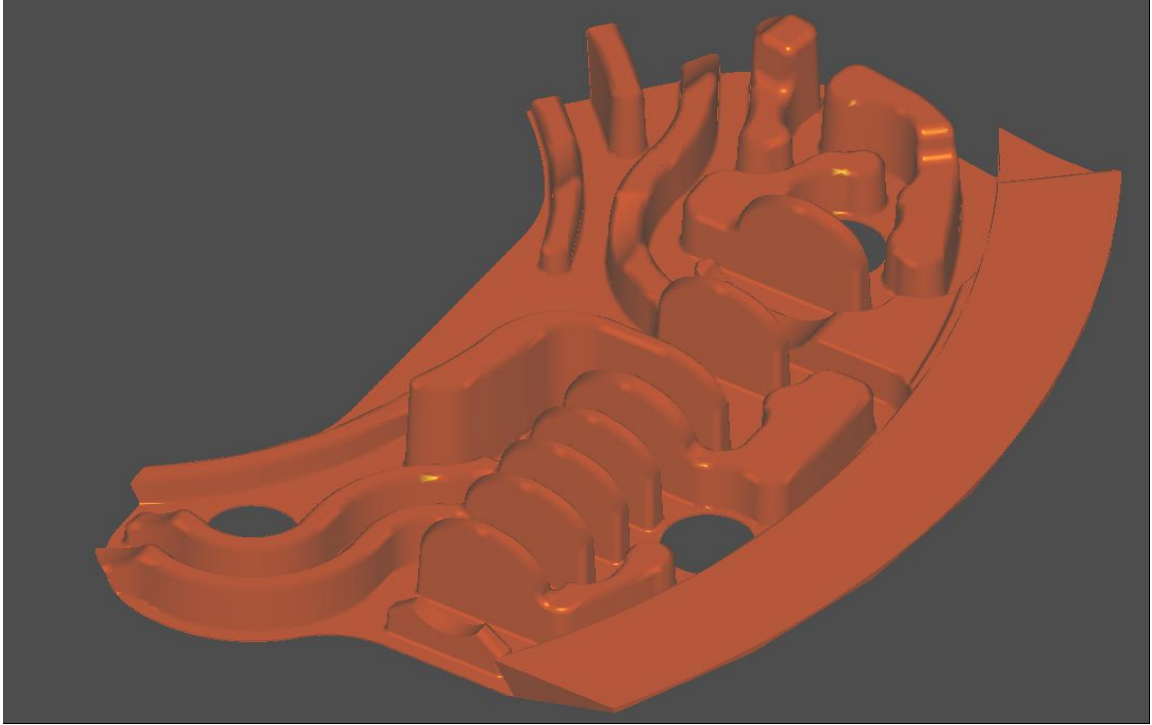
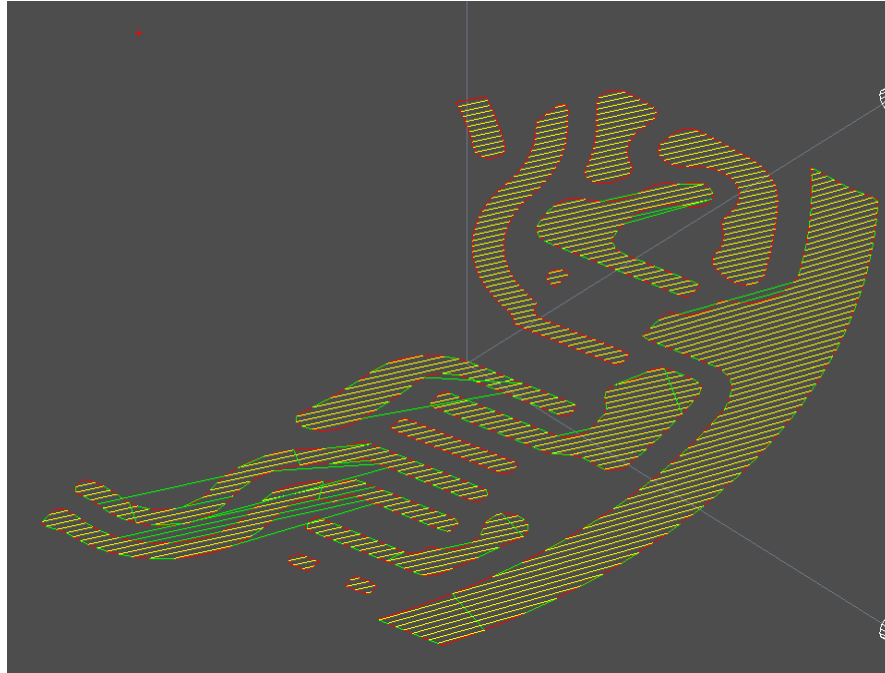


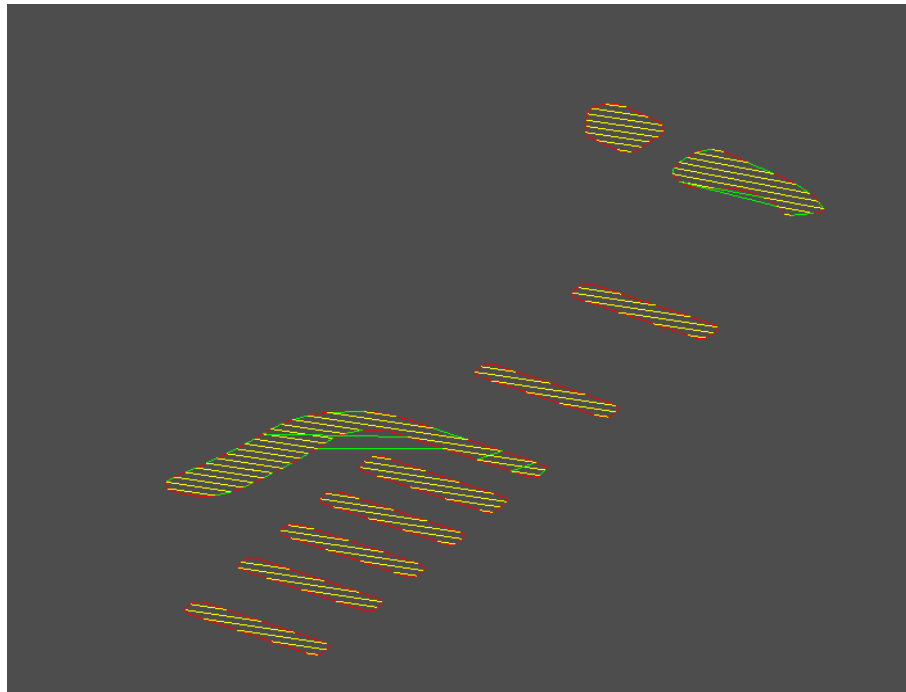
Figure 5.4. Original Spartan Part

Figure 5.4 is the original Spartan part on which slicing is performed at a certain height followed by 2D path planning using Zigzag method. Figures 5.5(a), (b) show the zigzag path on bottom most and topmost slices respectively. The green lines in Figure 5.6 represent the non-depositing paths and the yellow lines show the depositing paths. The track width and the height are user defined.





(a) Zigzag path on the bottom-most 3D layer of Spartan



(b) Zigzag path on top slice of Spartan

Figure 5.5. Zigzag at different levels on spartan

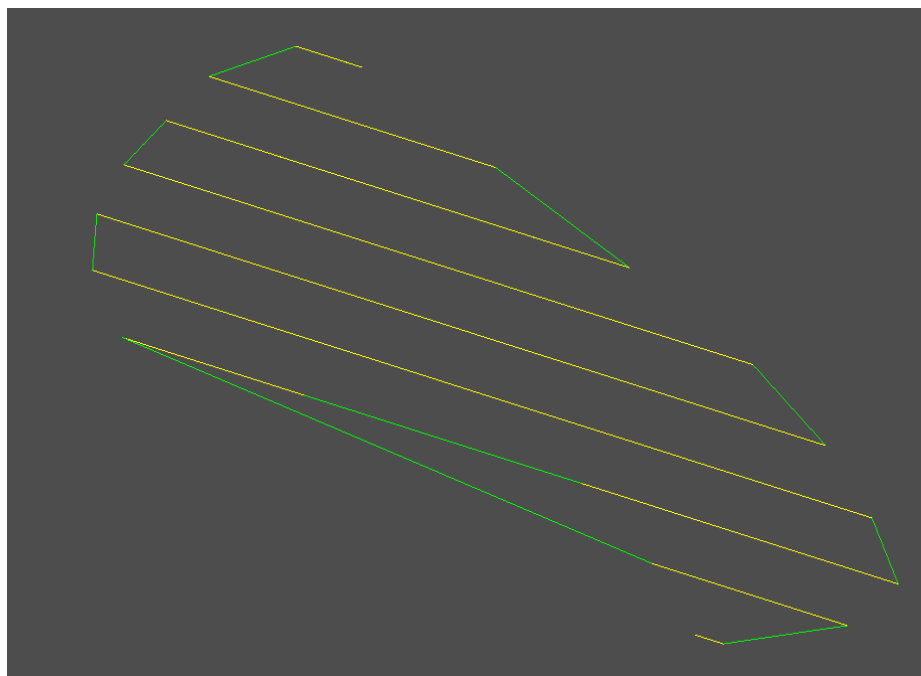


Figure 5.6 Zigzag illustration on spartan

## 6. CONCLUSIONS

The multi-axis deposition system can potentially make solid freeform fabrication very attractive to industry. The slicing of CAD models based on analysis of topological information between neighboring layers for such machines is presented. The method presented provides the following characteristics:

1. The slicing direction change can be identified by checking the topological information.
2. An optimal building sequence can be determined using collision check.
3. The overhang structure can be fabricated by rotating the slicing direction.

The cusp height problem is resolved to a great extent using multi-axis slicing. The layer thickness and angle adjustment helps in reducing the staircase effect. Building overhang structures is made easy. Since, building thin transition walls is not only difficult but inefficient for heavy structures. It also offers very little resistance to high temperatures. The overhang structures have a better deposition process due to the direction changing and decision making of creating a split surface.

The potential advantage realized by this new method is critical to the layered manufacturing industry. In particular, users of 3D layer deposition systems may benefit from enormous savings in fabrication time.

By using topological information between neighboring layers, the multi-axis slicing process integrates the concepts of the “3-D” layer or decomposition of an object to make the slicing result accurate. The entire process is automatically driven by local geometry information without human interference. The algorithm is implemented on a geometry kernel, therefore it is very easy to extend its application on any geometry format including STL.

## BIBLIOGRAPHY

- [1] Das, Suman; Harlan, Nicole; Beaman, Joseph and David Bourell, "Selective Laser Sintering of High Performance High Temperature Metals", Proceedings of Solid Freeform Fabrication, Austin, TX, 1996, pp 89-96.
- [2] Fodran, Eric; Koch, Martin and Menon, Unny, "Mechanical and Dimensional Characteristics of Fused Deposition Modeling Build Styles", Solid Freeform Fabrication Proceedings, 1996, pp 419-442.
- [3] Jacobs, P. F.," Stereolithography and Other RP&M Technologies: From Rapid Prototyping to Rapid Tooling" Society of Manufacturing Engineers, 1995.
- [4] McAlea, Kevin and Hejmadi, Uday," Selective Laser Sintering of Metal Molds: The RapidTool (TM) Process", Solid Freeform Fabrication Proceedings, 1996, pp 97-104.
- [5] Pope, Matthew J.; Patterson, Mark C.L. Patterson; Zimbeck, Walter and Fehrenbacher, Mark, "Laminated Object Manufacturing of Si<sub>3</sub>N<sub>4</sub> with Enhanced Properties", Solid Freeform Fabrication Proceedings, 1997, p 529-536.
- [6] Hofmeister, W., M. Griffith, M. Ensz, J. Smugeresky, Solidification in Direct Metal Deposition by LENS Processing, JOM-Journal Of The Minerals Metals & Materials Society, v. 53(#9) pp. 30-34 Sep 2001.
- [7] Laeng, J.; Stewart, J.G.; and Liou, F.W., "Laser Metal Forming Processes And The Application In Rapid Prototyping of Metallic Parts", Proceedings of the 2nd International Conference on Advanced Manufacturing Technology, Johor Bahru, Malaysia, August 2000a.

- [8] Laeng, J.; Stewart J.G.; and Liou, F.W., “Laser Metal Forming Processes for Rapid Prototyping – A Review,” *International Journal of Production Research*, Vol.38, No.16, pp.3973, 2000b.
- [9] Pandey, Pulak Mohan; Reddy, N. Venkata and Dhande, Sanjay G., “Slicing procedures in layered manufacturing: a review”, *Rapid Prototyping Journal*, Vol. 9 No. 5 2003, pp.274-288.
- [10] Dolenc, A and Mäkelä, I, “Slicing procedures for layered manufacturing techniques”, *CAD*, Vol. 26, Feb. 1994, pp.119-126.
- [11] Kulkarni, Prashant and Dutta, Debasish, “An accurate slicing procedure for layered manufacturing”, *CAD*, Vol.28, No.9, 1999, pp.683-397.[12] Kumar, Madhup and Choudhury, A. Roy, “Adaptive slicing with cubic path approximation”, *Rapid Prototyping*, Vol. 8. No. 4, 2002, pp.224-232.
- [13] Ma, Weiyin and He, Peiren, “An adaptive slicing and selective hatching strategy for layered manufacturing”, *Journal of Material Processing Technology*, 1999, pp.191-197.
- [14] Tata, Kamesh; Fadel, Georges; Bagchi, Amit and Aziz, Nadim, “Efficient slicing for layered manufacturing”, *Rapid Prototyping*, Vol. 4. No. 4, 1998, pp.151-167.
- [15] Luo, Ren C.; Chang, Yi Cheng and Tzou, Jyh Hwa, “The development of a new adaptive slicing algorithm for layered manufacturing system”, *Proceedings of the 2001 IEEE International Conference on Robotics & Automation*, Seoul, Korea, May 21-26, 2001.
- [16] Yang, Y.; Fuh, J.Y.H.; Loh, H. T. and Wong, Y. S., “A volumetric difference-based adaptive slicing and deposition method for layered manufacturing”, *Journal of Manufacturing and Science*, Vol.125, Aug. 2003, pp.586-594.

- [17] Singh, Prabhjot; Dutta, Debasish, “Multi-Direction Slicing for Layered Manufacturing”, *Journal of Computing and Information Science in Engineering*, June, 2001, Vol. 1, pp.129-142.
- [18] Zhang, J.; Ruan, J.; and Liou, F.W. “Process Planning for a Five-Axis Hybrid Rapid Manufacturing Process”, *Proceedings of the Eleventh Annual Solid Freeform Fabrication Symposium*, Austin, TX, pp. 243., August 2000.
- [19] Zhang, Jun and Liou, F.W. “Adaptive Slicing for a Five-Axis Laser Aided Manufacturing Process,” *Proceedings of the 2001 ASME Design Automation Conference*, Pittsburgh, Pennsylvania, September 9-12, 2001.
- [20] Ruan, J., Eiamsa-ard, K., and Liou, F.W., 2005, “Automatic Process Planning and Toolpath Generation of A Multi-Axis Hybrid Manufacturing System,” *SME Journal of Manufacturing Processes*, Vol. 7, No. 1, pp 57-68.
- [21] Ruan, Jianzhong; Tang, Lie; Sparks, Todd E; Landers, Robert G. and Liou, F.W., “Direct 3D Layer Metal Deposition and Toolpath Generation”, *Proceedings of the 2008 ASME International Design Automation Conference*, New York, USA, August, 3-6, 2008, *Paper No. DAC-50062*.
- [22] Koch, J.L. and Mazumder, J., *Rapid Prototyping by Laser Cladding*, *The International Society for Optical Engineering*, vol. 2306, 1993, p. 556-eoa.
- [23] Keicher, D.M., Miller, W.D., Smugeresky, J.E. and Romero, J.A., “Laser Engineered Net Shaping (LENS): Beyond Rapid Prototyping to Direct Fabrication” , *Proceeding of the 1998 TMS Annual Meeting*, San Antonio, Texas, USA, p. 369 - 377
- [24] Kreutz, E. W., Backes, G., Gasser, A. and Wissenback, K., “Rapid Prototyping with CO<sub>2</sub> Laser Radiation,” *Applied Surface Science*, vol. 86, 1995, p. 310-316.

- [25] Lewis, G. K., Nemec, R., Milewski, J., Thoma, D.J., Cremers, D., and Barbe, M., "Directed Light Fabrication," *ICALEO* , 1994, p.17-26.
- [26] McLean, M. A., Shannon, G. J. and Steen, W. M., "Laser Generating Metallic Components", *SPIE*, Vol. 3092, 1997, p. 753-756.
- [27] Pelletier, J.M. and Sahour, M.C., "Influence of Processing conditions on Geometrical Features of Laser Claddings Obtained by Powder Injection," *J of Materials Science*, vol. 28, 1993, p. 5184-5188.
- [28] Calvalho, P.A, Braz, N., Pontinha, M.M., Ferreira, M.G.S., Steen, W.M., Vilar, R. and Watkin, K.G., "Automated Workstation for Variable Composition Laser Cladding-- Its Use For Rapid Alloy Scanning," *Surface and Coatings Technology*, vol. 72, 1995, p.62-70



## VITA

Divya Kanakanala was born on September 19, 1986 in Hyderabad, India. She completed her secondary education at Kendriya Vidhyalay High School, Hyderabad, India. She received the degree of Bachelor of Engineering in Computer Science from Chaitanya Bharathi Institute of Technology, Hyderabad, India affiliated with the Osmania University, India in May 2007. She worked for Wipro technologies, Hyderabad, India in August 2007. She joined the Master of Science program in Computer Science at the Missouri University of Science and Technology, Rolla in August 2008 and received her Master of Science degree in Computer Science in May 2009. Her research with Dr. Frank Liu at the Missouri University of Science and Technology, Rolla has concentrated on Multi-Axis slicing for direct laser deposition.